Limitation of the fusion cross section for the $^{12}C+^{11}B$ system at $E_{c.m.}=36.5$ and 41.7 MeV

M. Kistryn, L. Jarczyk, B. Kamys, A. Magiera, Z. Rudy, and A. Strzałkowski
Institute of Physics, Jagellonian University, PL-30059 Cracow, Poland

R. Barnà, V. D'Amico, D. De Pasquale, A. Italiano, and M. Licandro
Dipartimento di Fisica, Università di Messina, and Istituto Nazionale di Fisica Nucleare, Sezione di Catania, Gruppo collegato di Messina, I-98166 Messina, Italy

(Received 8 March 1996)

Inclusive spectra of protons, α particles, and heavy ejectiles as well as coincidence spectra of protons and α particles with heavy ejectiles were measured for $^{12}C+^{11}B$ system at several angles and at two laborabory energies of ^{11}B: 70 and 80 MeV. A Hauser-Feshbach model analysis was performed for inclusive and coincidence spectra to extract the fusion cross section values 800 $\pm$ 50 mb and 750 $\pm$ 50 mb at E_{lab} 70 and 80 MeV, respectively. These values are in agreement with the limitation of the fusion imposed by entrance channel conditions and by properties of the compound nucleus, in contradiction to results of earlier investigations which suggested an anomalous energy dependence of the fusion. [S0556-2813(96)02610-6]

PACS number(s): 25.70.Jj, 24.60.Dr, 25.70.Gh

I. INTRODUCTION

Fusion process plays an important role in nuclear collisions in a very broad range of energies. The energy dependence of the fusion cross section for light heavy-ion systems exhibits different behavior in three beam energy regions [1]: In the low energy region—$E_{c.m.}$ smaller than approximately two heights of the Coulomb barrier (''region I'')—the fusion cross section is proportional to $1/E_{c.m.}$. This is well understood in terms of the barrier penetration effects. At higher energies (''region II'') the fusion cross section decreases substantially due to a dynamical competition between fusion and peripheral reactions mediated by both: properties of the compound nucleus and specific features of the entrance channel. A highest energy range (''region III'') is characterized by a rapid falloff of the fusion cross section [2], due to the lack of fulfillment of conditions for the formation of a compound nucleus at higher angular momenta.

A typical example of such an energy dependence is presented in Fig. 1(a) for $^{18}O+^{12}C$ [3–6]. In the case of the $^{12}C+^{11}B$ system, however, the experimental values of the fusion cross sections at energies from region II stay according to results of Ref. [7] almost constant as shown in Fig. 1(b) instead of decreasing with energy. Such an unusual energy dependence of the fusion cross section in this energy region seems to be in contradiction with the distinct monotonic decrease of the fusion cross section predicted by different fusion models. It is interesting to stress that an anomalous behavior was observed for this system also in another reaction. Experimentally it was found that elastic and inelastic proton transfer has a very large probability [8–10]. What is more, the energy dependence of the elastic transfer cross section shows an anomaly, which in the direct reaction model analysis could be only simulated by introducing the unphysical assumption of an energy-dependent spectroscopic factor of ^{12}C [8]. This stimulates suspicion that both anomalies, in the fusion cross section as well as in elastic transfer, could have some common origin, being somehow coupled through the mechanisms of both processes.

Having this in mind we performed in the present work a precise measurement of the fusion cross section for the $^{12}C+^{11}B$ system at two energies $E_{c.m.}=$ 36.5 and 41.7 MeV, where a distinct decrease of the the fusion cross section is expected according to fusion models. Usually the fusion

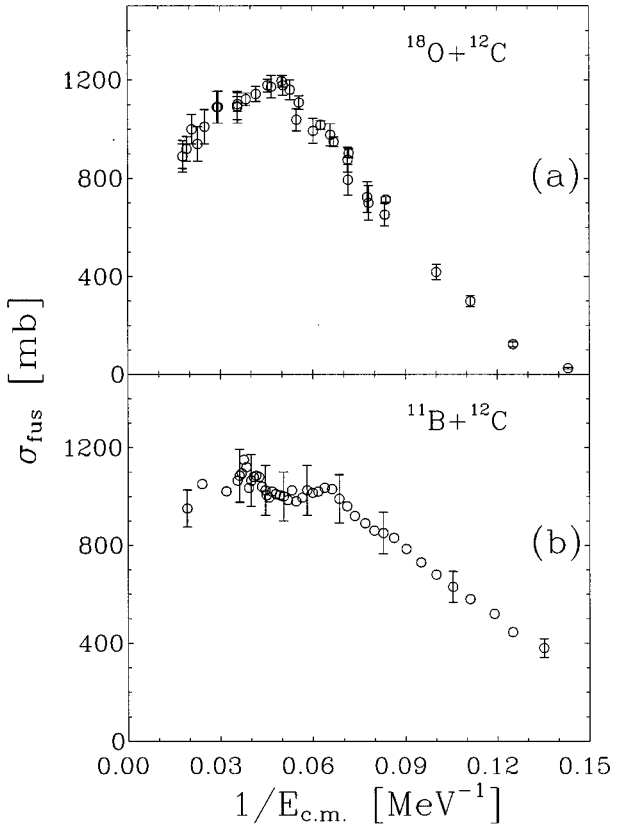

FIG. 1. Experimental fusion cross section as a function of a reciprocal c.m. energy of colliding nuclei (a) for $^{18}O+^{12}C$ ([3–6]), (b) for $^{12}C+^{11}B$ system [7].

cross section is extracted from the inclusive spectra of the evaporation residua. However, for light heavy-ion collisions at higher energies this may lead to confusion due to the considerable contribution from direct processes. To avoid any ambiguity the inclusive measurements of the energy spectra (of both heavy nuclei and light particles) were supplemented by coincidence measurements of protons or α particles with heavy ejectiles.

The results of the measurements were compared with Hauser-Feshbach model predictions. The fusion cross section was the only free parameter in this analysis while the values of the other parameters of the model were taken from earlier investigations of fusion reactions published in the literature.

The experimental procedure and the results are presented in Sec. II of the paper. The description of the statistical model analysis and discussion of the limitation of the fusion cross section follows in Sec. III, while a summary with conclusions is provided in Sec. IV.

II. EXPERIMENTAL PROCEDURE AND RESULTS

The measurements have been performed at the Laboratorio Nazionale del Sud (LNS) in Catania, Italy. The experiment has been done with the ^{11}B ion beams of 70 MeV and 80 MeV laboratory energies from the 13 MV SMP Tandem Van de Graaff accelerator. The ^{12}C foil with a thickness of 0.2 mg/cm^2 served as the target. The measurements were performed using ΔE-E counter telescopes for particle identification. Inclusive energy spectra for light particles (protons and α particles) and heavy reaction products as well as coincidence energy spectra of light particles with heavy ejectiles have been measured in a broad angular range. For the measurement of the inclusive energy spectra of the B, C, N, O, F, and Ne nuclei, an ionization chamber was used as the ΔE counter and the semiconductor position-sensitive detector as the E counter [8]. The range of laboratory angles was from 5° to 27°, covered in 2° steps. The overall energy resolution of the telescopes was about 500 keV while that of the ΔE counter was sufficient to allow an unambiguous charge identification of the detected reaction products. For the determination of the energy spectra of protons, α particles, Li and Be nuclei the δE-ΔE-E telescopes consisting of Si surface barrier detectors of thickness 10-300-3000 μm or 50-400-3000 μm, with a solid angle of 0.3 msr were used [11]. The energy resolution of these telescopes was around 200 keV. Also in this case a very good charge identification has been obtained. The measurements covered the range of laboratory angles from 10° to 110°, divided into 5° steps at $E_{\rm lab}(^{11}\mathrm{B}) = 70$ MeV, and the angular range from 5° to 34°, divided into 1° steps at 80 MeV.

In all the measurements the accuracy of the energy calibration was about 300 keV. The detection energy threshold depended on the experimental conditions and was within the range of 5 MeV (for Li) to 25 MeV (for Ne) for heavy ejectiles and about 8–12 MeV for light particles. The absolute values of the cross sections were determined from the measured counting rates, the target thickness, the solid angles of detecting systems, and the integrated beam charge. The uncertainty of the absolute normalization was estimated to be about 7%.

The ejectiles with different Z in the range 1–10 were identified on the basis of the two-dimensional energy plots. In Fig. 2 an example of such plot is shown for a measurement with the δE-ΔE-E detector system.

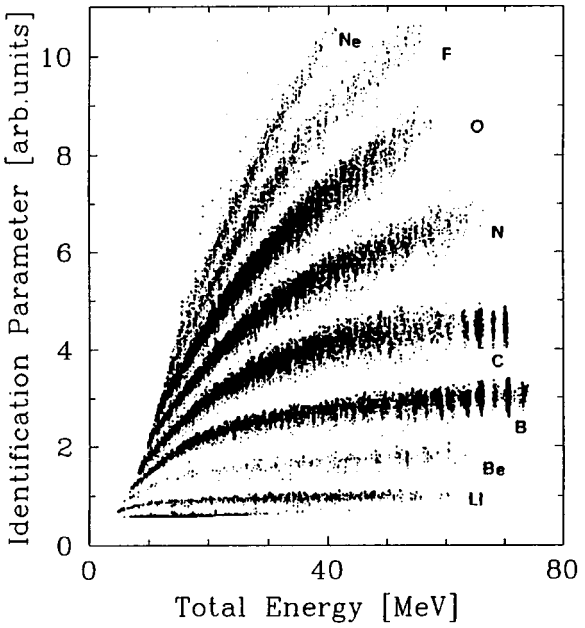

FIG. 2. Two-dimensional plot used for particle identification. On the horizontal axis the total energy $E_t = \delta E + \Delta E + E$ is shown, on the vertical one an identification parameter equal to $\delta E \times E_t$.

Typical experimental energy spectra of all the reaction products from protons and α particles up to Ne nuclei are shown in Fig. 3. According to qualitative features the spectra can be grouped into three categories. One group is characterized by the presence of a broad bump near the energy $E_c = \frac{1}{2} m_{\rm ejectile} v^2_{\rm c.m.}$ where $v_{\rm c.m.}$ is the center-of-mass velocity (in Fig. 3 arrows labeled c), which can be attributed to the reaction proceeding through the compound nucleus formation. Another group of the energy spectra exhibits discrete peaks near the energy $E_b = \frac{1}{2} m_{\rm ejectile} v^2_{\rm beam}$ corresponding to the beam velocity (in Fig. 3 arrows labeled b), which can be explained as caused by direct reactions. The energy spectra of Ne, F, and O nuclei belong to the first group. The energy spectra of Li and Be nuclei possess characteristic features of the second type. In the energy spectra of B, C, and N nuclei one can find signatures of both groups described above, which suggests contributions of both reaction mechanisms.

The two-dimensional coincidence energy spectra of protons or α particles with heavy ejectiles were measured for six angular configurations. Ejectiles were detected and Z identified by five Si telescopes positioned on both sides of the beam. Two of them (10-300-3000μm, for heavy ejectiles), were placed at $-7°$ and $-14°$, and three other (50-400-3000μm, for light particles) were at $+7°$, $+14.4°$, and $+21.6°$.

In Fig. 4 examples of these coincidence spectra are shown which exhibit all typical features observed in the present experiment. For coincidence energy spectra of α particles with Li ejectiles one can notice a strong grouping of events on the three-body kinematical curve of the ^{12}C(^{11}B, α ^{7}Li)^{12}C$_{\rm g.s.}$ reaction. The coincidence pattern of α particles with heavy ejectiles (nuclei C–F) and that of protons with heavy ejec-

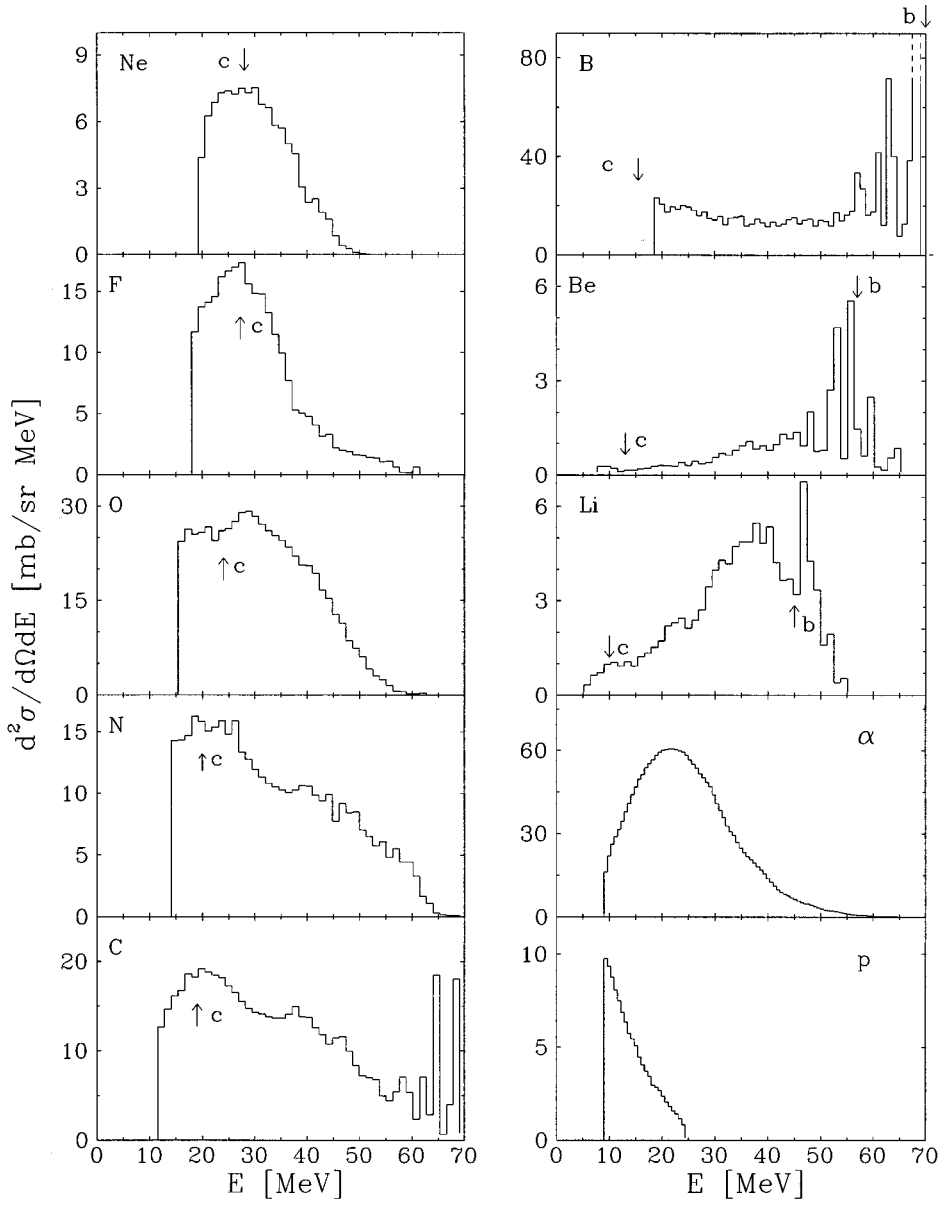

FIG. 3. Experimental energy spectra (LAB) of various products originating from the interaction of the ^{11}B projectiles with the ^{12}C target nuclei at 70 MeV laboratory energy. The energy spectra of heavy ejectiles are measured at 7° and those of light particles (α,p) at 10°. Arrows labeled *b* and *c* show the energy of the particle moving with the beam velocity and center-of-mass velocity, respectively. For ejectiles heavier than the beam particle ^{11}B the arrow *b* lies outside the plot.

tiles exhibit a completely different structure. All the events lie inside the three-body kinematics area, which suggests their origin in more than three-body reactions. An intermediate behavior is shown in the α-B coincidence spectrum, where many events lie in a strip around the three body kinematical curve, grouped in few peaks, but there is also quite a large amount of many-body reaction events.

III. STATISTICAL MODEL ANALYSIS

From an examination of the qualitative features of the experimental spectra, discussed in the previous section, one can conclude that the nuclear reactions in the studied nuclear system $^{12}C+^{11}B$ proceed via direct as well as compound nucleus mechanisms. We focus our attention on the processes connected with the formation of the compound nucleus. To describe them the statistical model formalism was applied in the frame of the Hauser-Feshbach model [12]. This model contains several parameters which should be fixed in a reliable, unambiguous way. The procedure used for this purpose is described in the first subsection, Sec. III A. Results of the calculations of inclusive and coincidence energy spectra are compared with the experimental data in the second subsection, Sec. III B. Various models for limitation of the fusion cross section are discussed in the third subsection, Sec. III C, and their predictions are compared with the experimental fusion cross section obtained in the present experiment.

The calculations were performed with the aid of the computer code PACE-2 [13] modified by Kistryn [14] to allow extraction of coincidence spectra of the evaporated particles: (α,p,n) and evaporation residua.

A. Parameters used in the Hauser-Feshbach model calculations

The main ingredients of the Hauser-Feshbach model are the probability of compound nucleus formation and the prob-

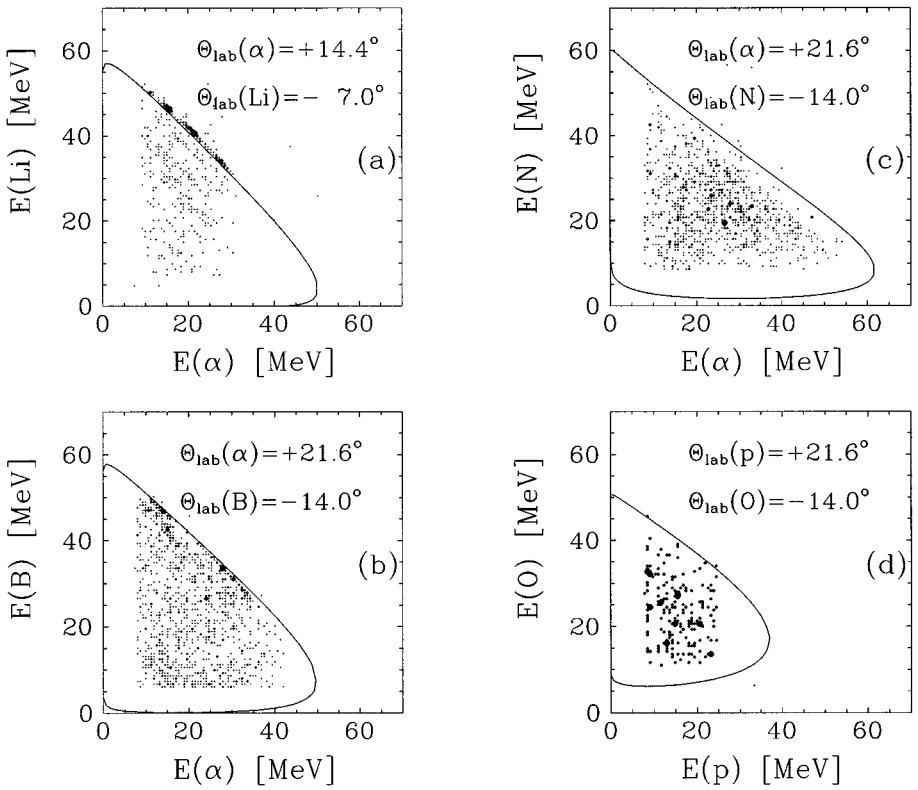

FIG. 4. Two-dimensional energy spectra for (a) α-Li, (b) α-B, (c) α-N, and (d) p-O coincidences. The solid lines show kinematical curves for (a) ^{12}C(^{11}B, α ^{7}Li)^{12}C $_{g.s.}$, (b) ^{12}C(^{11}B, α ^{11}B)^{8}Be, (c) ^{12}C(^{11}B, α ^{15}N)α, and (d) ^{12}C(^{11}B, p-^{17}O)^{5}He processes.

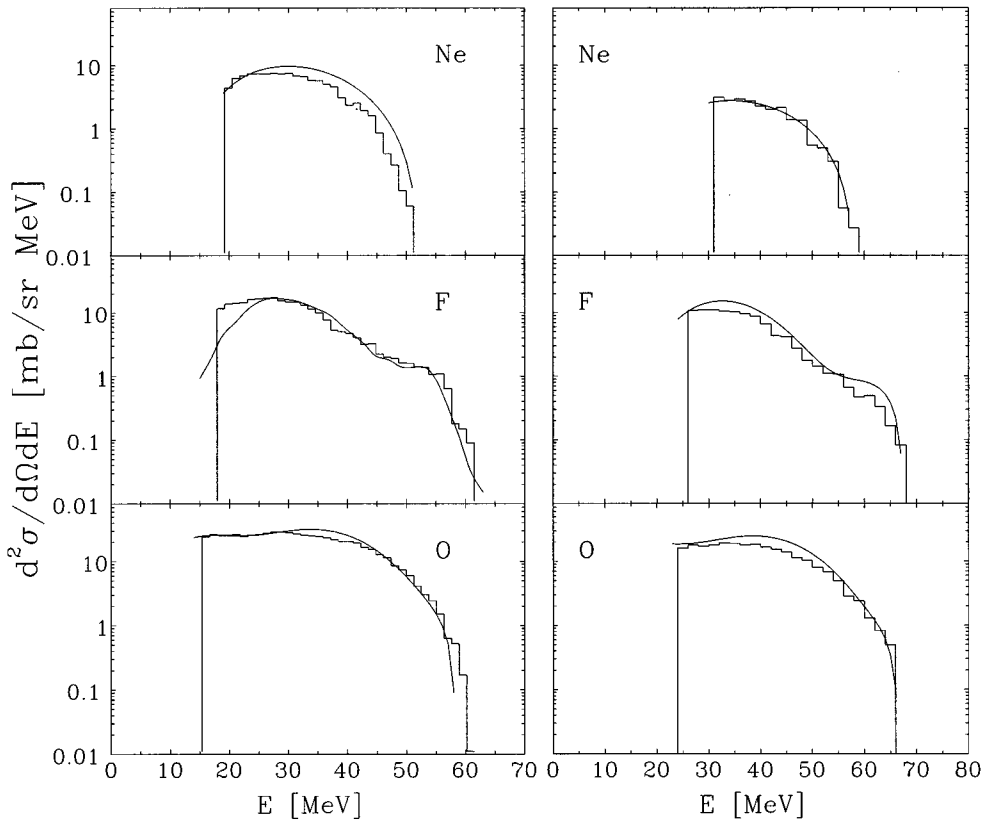

FIG. 5. Comparison of the experimental energy spectra (histograms) with the Hauser-Feshbach model calculations (solid lines) for the Ne, F, and O nuclei emitted at θ_{lab} = 7° at E_{lab}=70 MeV (left side) and E_{lab}=80 MeV (right side). The sharp low-energy cut in the experimental data is due to the detection energy threshold.

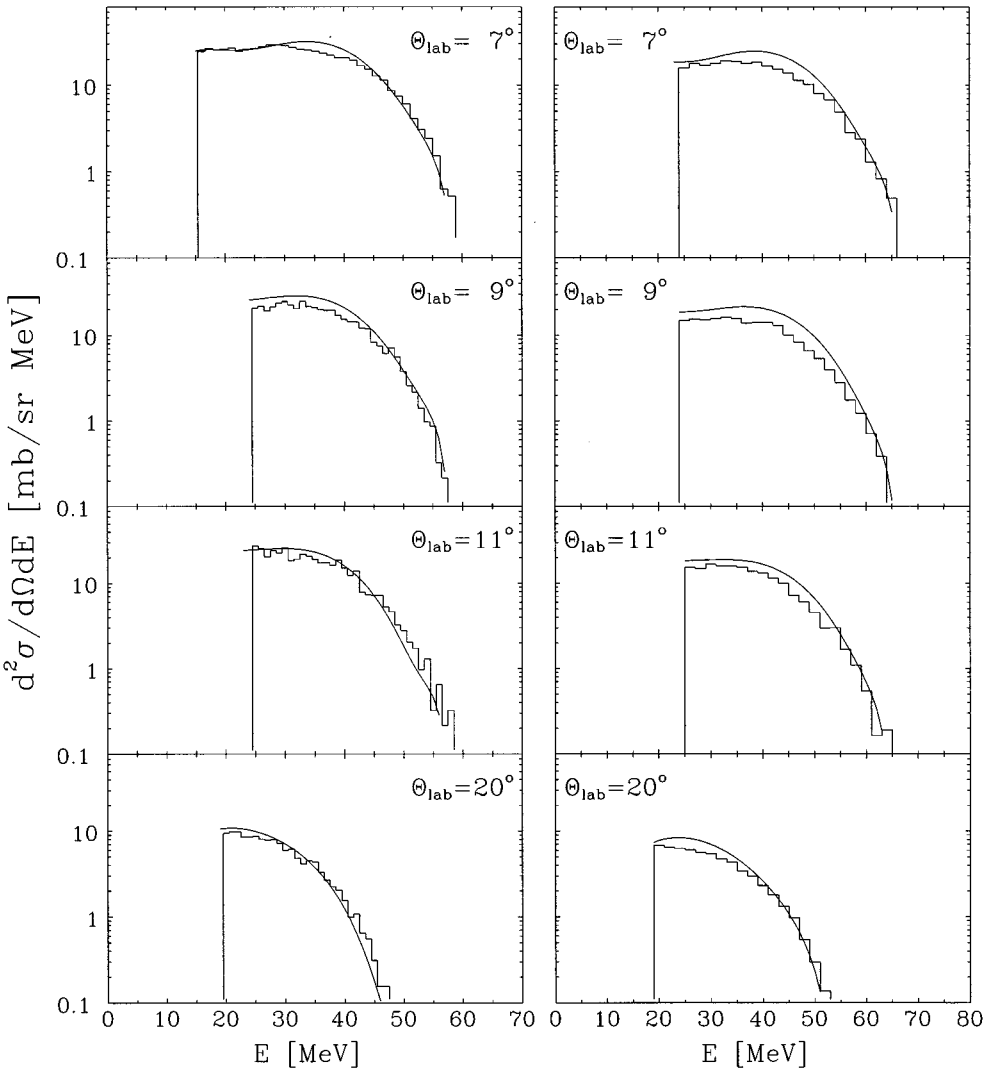

FIG. 6. Comparison of the experimental energy spectra (histograms) with the Hauser-Feshbach model calculations (solid lines) for O nuclei produced at different laboratory angles for both beam energies ($E_{\rm lab}$=70 MeV, left side, $E_{\rm lab}$=80 MeV, right side). The sharp low-energy cut in the experimental data is due to the detection energy threshold.

ability of evaporation of light particles from the compound nucleus. These probabilities are determined by transmission coefficients $l_{\rm fus}$, in the entrance and exit channels, the density of states of nuclei produced during various stages of the evaporation process, and by the fusion cross section. The transmission coefficients as well as the density of nuclear levels depend on parameters of the phenomenological formulas (of the optical model potentials and level density formulas, respectively). Thus the fusion cross section could be determined unambiguously as the only free parameter of Hauser-Feshbach model calculations by comparison of the calculated spectra of different ejectiles with the experimental ones.

The following prescription has been applied to fix values of the parameters of the model.

The optical model potentials which reproduce well the experimental data on the elastic scattering in the entrance and the exit channels were used. The transmission coefficients in the entrance channel were obtained with the optical model using the parameters from Ref. [8]. In the case of the exit channel the optical model calculations were performed employing potentials for protons and neutrons from the compilation of Perey and Perey [15] and for α particles those from Ref. [16].

At low excitation energies the existing experimental information on the energy (E^*) and spin (I) of individual levels was used [17,18]. At higher excitation energies (E^*) the commonly accepted Gilbert-Cameron parametrization of the level densities [19], given by the formula

$$\rho(E^*,I)=\frac{1}{24\sqrt{2}\sigma^3 a^{1/4}}\frac{\exp 2[a(E^*-\Delta)]^{1/2}}{(E^*-\Delta)^{5/4}} \times(2I+1)\exp\frac{-(I+1/2)^2}{2\sigma^2}, \quad (1)$$

with spin cutoff parameter

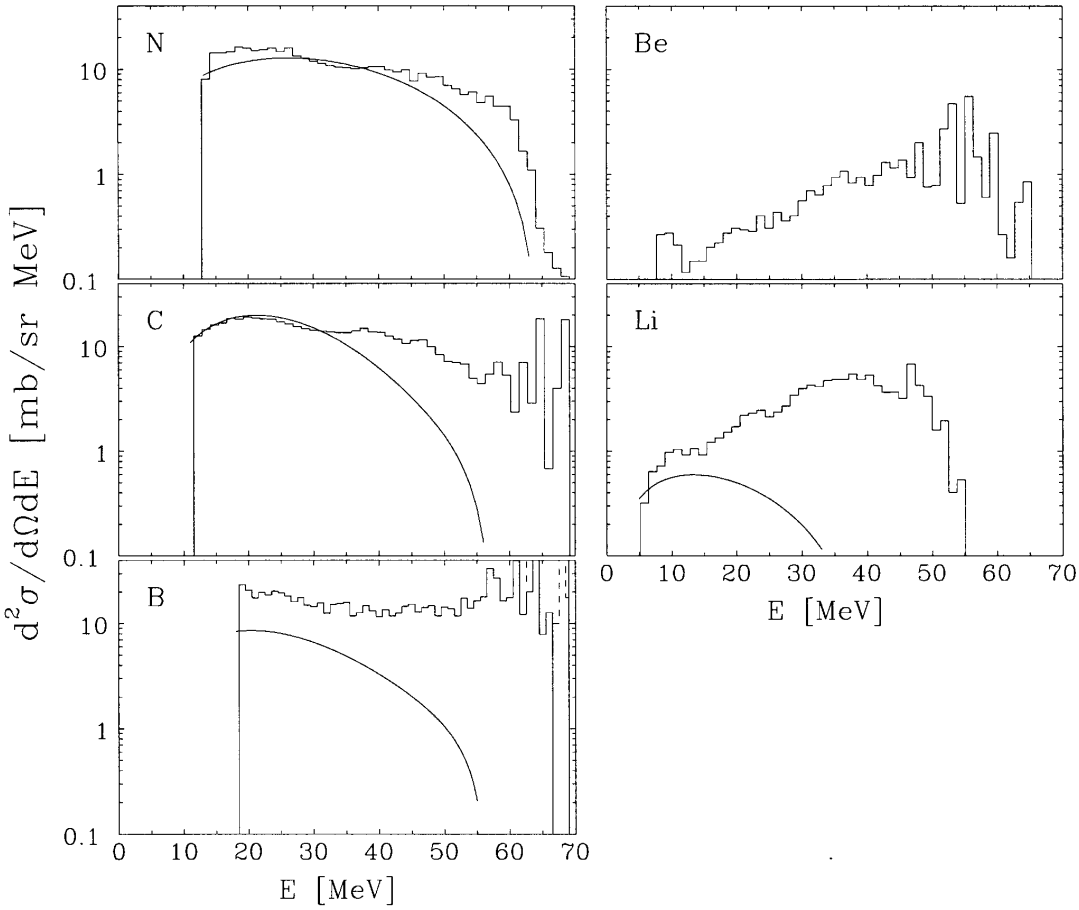

FIG. 7. Comparison of the experimental energy spectra (histograms) for the N, C, B, Be, and Li nuclei produced at θ_{lab} = 7° in the $^{12}C+^{11}B$ reaction at E_{lab}=70 MeV, with the Hauser-Feshbach model calculations (solid lines). In the case of beryllium, the HF model predictions are very small. The sharp low-energy cut in the experimental data is due to the detection energy threshold.

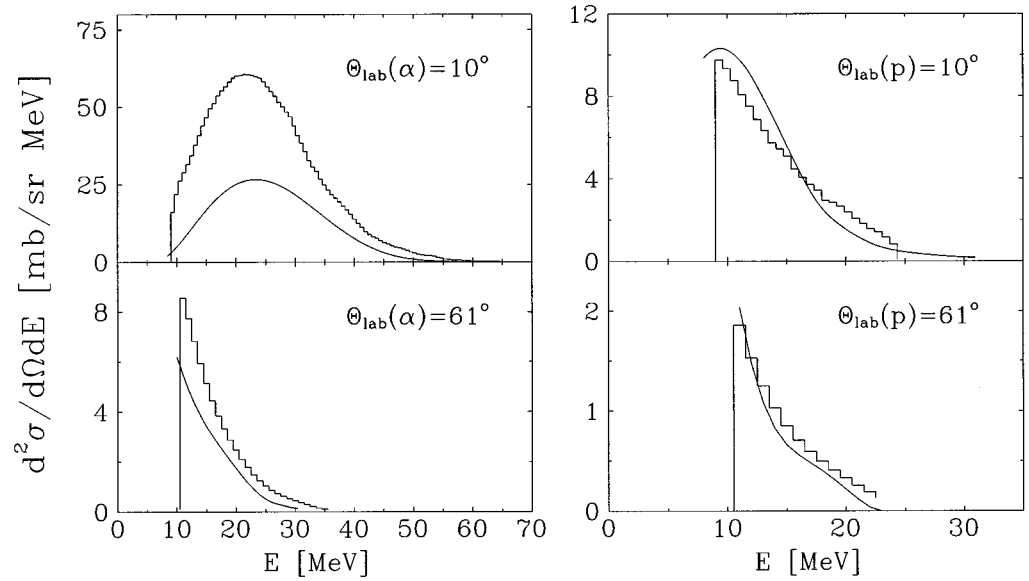

FIG. 8. Comparison of the experimental energy spectra (histograms) of α particles (left side) and protons (right side) measured at 10° and 61° with the Hauser-Feshbach model calculations (solid lines). The sharp low-energy cut in the experimental data is due to the detection energy threshold.

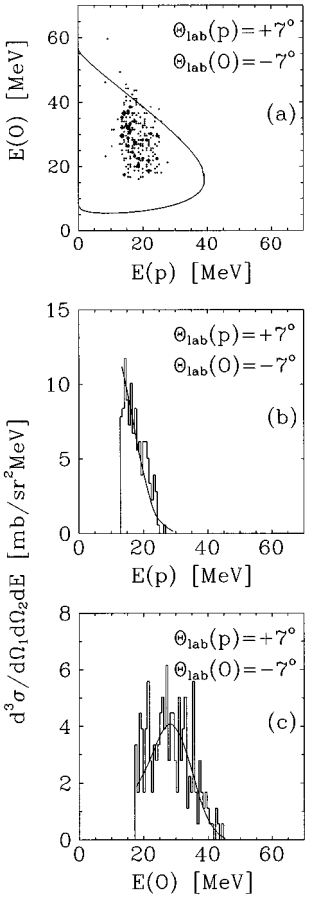

FIG. 9. Coincidence spectra of p and oxygen ejectiles emitted at angles $+7°$ and $-7°$, respectively. (a) Two-dimensional scatter energy plot; the solid line represents the kinematical curve for ^{12}C(^{11}B, ^{17}O p) ^{5}He with all particles in their ground states. (b) and (c) Comparison of Hauser-Feshbach model calculations (solid lines) with experimental coincidence energy spectra (histograms) for protons and O nuclei, projected on corresponding energy axes.

$$\sigma^2 = 0.0888[a(E^* - \Delta)]^{1/2} A^{2/3},$$

was accepted. This parametrization contains two basic parameters: the level density parameter a and pairing energy Δ.

The value of the level density parameter a was calculated according to the formula given in Ref. [19]:

$$a = A[0.00917(SZ + SN) + 0.142], \qquad (2)$$

with shell corrections for protons SZ and for neutrons SN published in Refs. [19,20] for nuclei with charge number Z and neutron number N both ≥ 9. For lighter nuclei we assumed a mean value of $(SZ+SN)$ equal to 6.2 MeV based on the known values of the shell corrections for nuclei with Z and N in range 9–12 (from ^{18}F up to the compound nucleus ^{23}Na). Values of the pairing energies Δ for nuclei with $Z,N \geq 9$ were taken from Ref. [19]. The method proposed in [21,22] was used to calculate pairing energy for lighter nuclei. The pairing energy calculated in this way for nuclei with $N,Z \geq 9$ agrees very well with values obtained using parameters of Ref. [19].

This procedure leaves the fusion cross section as the only parameter of the model to be extracted from the analysis.

B. The comparison of experimental energy spectra with model calculations

The values of the fusion cross section $\sigma_{\rm fus}$ were estimated at both energies by comparison of experimental inclusive energy spectra with the predictions of the Hauser-Feshbach model. The results for neon, fluorine, and oxygen ejectiles are especially significant in this procedure since the qualitative properties of their spectra, discussed in the previous section, suggest a dominant role of the compound nucleus mechanism. Furthermore, it is very unlikely that these ejectiles are produced by direct reactions, because such a mechanism must involve the transfer of many nucleons (five for ^{16}O and more for other ejectiles) from the ^{12}C target to the ^{11}B projectile. Such processes proceed with a very small cross section at the energies under investigation [23]. The excellent agreement between Hauser-Feshbach model calculations and the experimental spectra obtained for both beam energies and all measured angles confirms that the Ne, F, and O ejectiles are produced in compound nucleus processes only and can be used for the $\sigma_{\rm fus}$ cross section determination. The examples of experimental data for Ne, F, and O nuclei measured at $\theta_{\rm lab}=7°$ and at both beam energies are presented in Fig. 5 together with the Hauser-Feshbach model calculations performed with the obtained values of $\sigma_{\rm fus}$. The experimental spectra for oxygen nuclei for both beam energies and for different angles are compared with the Hauser-Feshbach model calculations in Fig. 6. The consistency of the analysis is confirmed by the fact that for ejectiles with $Z \leq 7$, where the considerable contribution of direct processes appears, the Hauser-Feshbach model prediction does not overcome the experimental values of the cross sections (see, e.g., Fig. 7). This is also true for the spectra of α particles whose examples are shown in Fig. 8, while the proton spectra presented in the same figure are well reproduced by Hauser-Feshbach model.

Within the above described procedure the values of fusion cross sections obtained from fits to the inclusive spectra of ejectiles with $Z > 7$ are 800 mb and 750 mb at $E_{\rm lab}$(^{11}B) of 70 MeV and 80 MeV, respectively. The fusion cross section accounts for about 50% of the total reaction cross section obtained from the OM calculations [9]. A similar ratio of fusion to reaction cross section was obtained for other comparable nuclear systems in the same energy range [24–29].

The stringent check of consistency of the Hauser-Feshbach model analysis was provided by comparing the results of the present coincidence measurements with model calculations. For the lighter ejectiles with $Z \leq 7$ the contribution of other (direct) reaction mechanisms prevents the determination of the fusion cross section from comparison of results of model calculations with the experimental spectra of ejectiles only. However, in these cases the measuring coincidences with the light ejectiles, α particles, and protons provides an excellent selection of compound nucleus mechanisms, presenting a stringent test of our fusion cross section determination. Very good agreement of the theoretical and experimental coincidence energy spectra has been obtained for proton-oxygen and proton-carbon coincidences for all

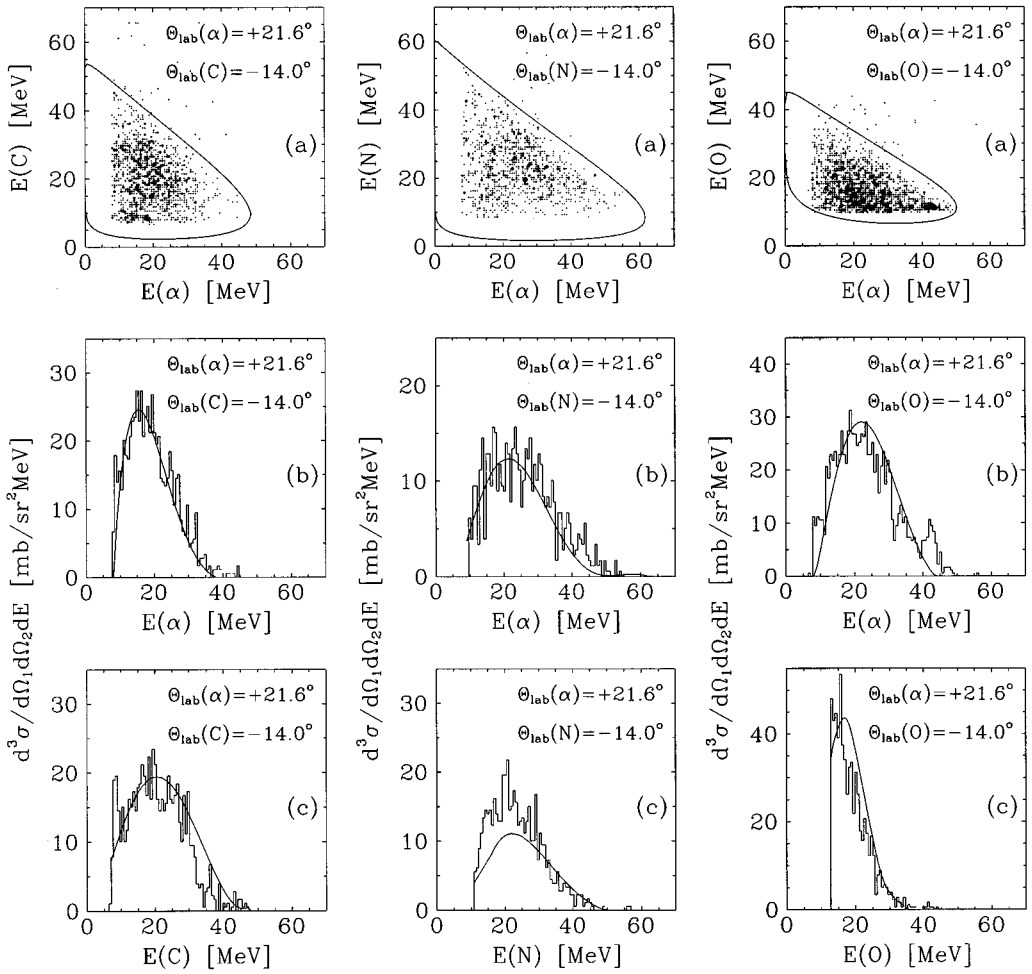

FIG. 10. Coincidence spectra of α particles with carbon (left column), nitrogen (middle column), and oxygen (right column) nuclei. (a) Two-dimensional scatter energy plot with kinematical curves ^{12}C(^{11}B, ^{14}C α) ^{5}Li, ^{12}C(^{11}B, ^{15}N α)α, and ^{12}C(^{11}B, ^{17}O α)d shown as solid lines. (b) and (c) Comparison of Hauser-Feshbach model calculations (solid lines) with experimental coincidence energy spectra (histograms) of α particles and heavy ejectiles (C, N, O) projected on the corresponding energy axes.

measured angular configurations. As an example the coincidence energy spectra for protons and oxygen nuclei at configuration $\theta_{\rm lab}(p)=+7°$ and $\theta_{\rm lab}({\rm O})=-7°$ are presented in Fig. 9. Figure 9(a) shows this coincidence pattern in the form of the two-dimensional scatter plot while projections of this plot on the proton or on the oxygen nuclei energy axes are presented in Figs. 9(b) and 9(c), respectively, together with the Hauser-Feshbach model predictions with values of fusion cross section determined from analysis of inclusive spectra.

A similar calculation within the framework of the Hauser-Feshbach model has been performed for the coincidence energy spectra of α particle with O, N, C, B, and Li nuclei. A very good description of the coincidence energy spectra by Hauser-Feshbach model calculations has been obtained for α-particle coincidences with oxygen, nitrogen, and carbon nuclei for all measured angular configurations. Typical examples of obtained results are shown in Fig. 10 for one angular configuration for α-O, α-N, and α-C coincidences, while the results for all measured angular configurations in the case of the α-C coincidences are presented in Fig. 11.

In contradistinction to these results the α-B and α-Li coincidence energy spectra are not entirely described when assuming the presence of compound nucleus processes only. As can be seen from Figs. 12(b) and 12(c) the Hauser-Feshbach model calculations underestimate the experimental values for α-B coincidence spectra in angular configuration $+7°$ / $-7°$. The same effect was observed for all angular configurations for α-B and α-Li coincidence energy spectra. This indicates the large contribution of direct processes in these reactions. Such processes could proceed, e.g., through the formation of unstable states of ^{15}N with their consecutive decay into an α-B channel. Selective grouping of coincidence events on the kinematical line corresponding to the ^{12}C (^{11}B,α ^{11}B) ^{8}Be$_{\rm g.s.}$ reaction, visible in Fig. 12(a), confirms this conclusion. Similar sequential processes appear also in α-Li coincidences; see Fig. 4(a).

The large contribution of direct reaction processes observed also in some inclusive spectra (see Fig. 7), can account for the difference between the optical model prediction of the total reaction cross section and fusion cross section following from the Hauser-Feshbach model analysis.

In order to check the consistency of the performed analysis the calculations were done with the fusion cross section values varied inside of the experimental cross section nor-

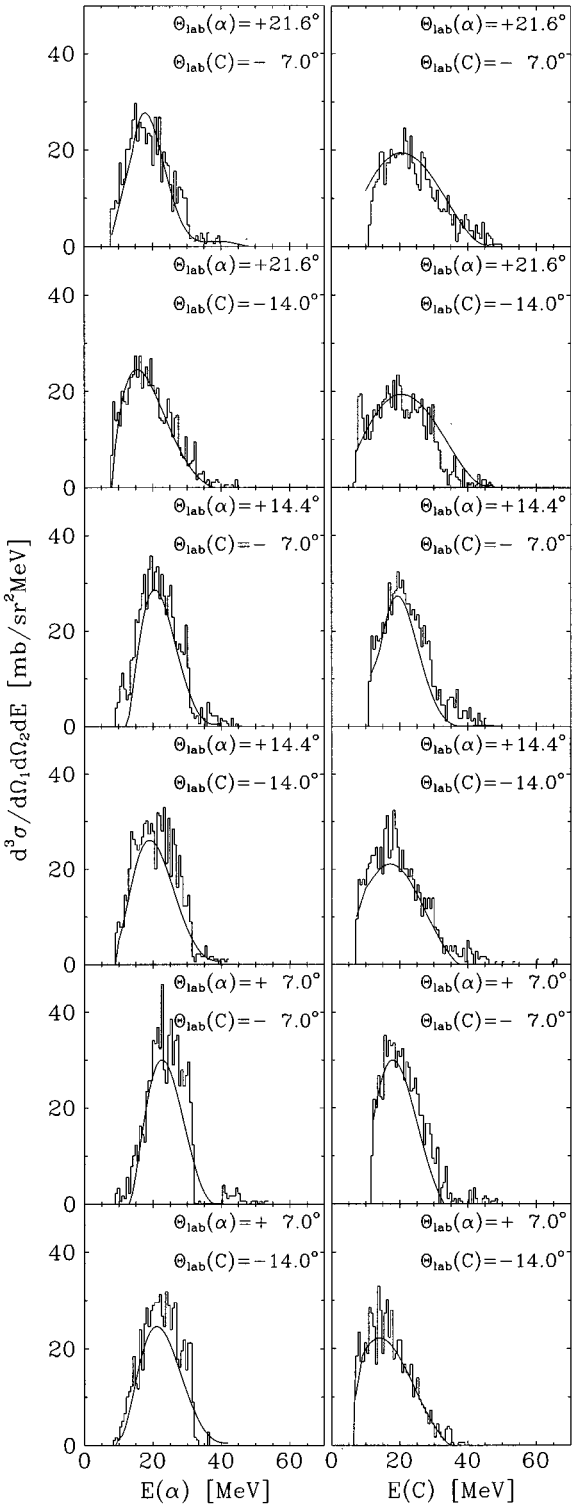

FIG. 11. Comparison of the experimental results (histograms) for α-C coincidences at different angular configurations with the Hauser-Feshbach model calculations (solid lines). Coincidence energy spectra are projected on the α particle energy axis (left column) and on the carbon nuclei energy axis (right column).

malization errors ± 50 mb. As can be seen from Fig. 13 the results of such calculations lead to the spectra—both inclusive as well as coincidence ones—with absolute values well outside of those obtained from experiment. This indicates

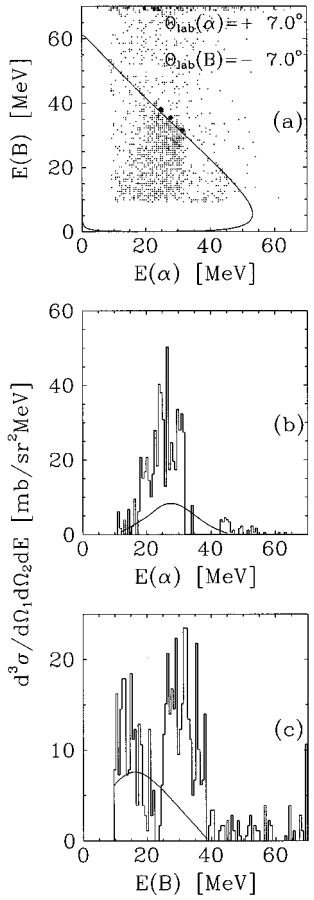

FIG. 12. Coincidence spectra of α particles and B nuclei. (a) Two-dimensional scatter energy plot; the solid line represents the kinematical curve of the ^{12}C(^{11}B,α ^{11}B)^{8}Be$_{\text{g.s.}}$ reaction. (b) and (c) Comparison of Hauser-Feshbach model calculations (solid lines) with experimental coincidence energy spectra (histograms) for α particles and B nuclei, projected on the corresponding energy axes.

that the model analysis introduces no additional inaccuracy to the determined values of the fusion cross section, being thus 800 ± 50 mb and 750 ± 50 mb at E_{lab}(^{11}B) of 70 MeV and 80 MeV, respectively.

C. Entrance channel and compound nucleus limitation of the fusion cross section

The results obtained in the present work are presented in Fig. 14 (solid squares) together with results of Refs. [7,42] obtained in a broad energy range. These results should be confronted with fusion model predictions. At higher energies there arise factors limiting the fusion probability. According to different models they could be attributed either to properties of entrance channel as, e.g., in Refs. [30–36] or to the features of the compound nucleus, e.g., Refs. [37–40].

Among the models assuming the entrance channel limitation of the fusion cross section two main ideas were developed: The idea of the ''critical distance'' which has to be reached by colliding nuclei in order to form the compound nucleus [31], and the idea of the ''critical angular momentum'' at which the ''pocket'' in the effective potential van-

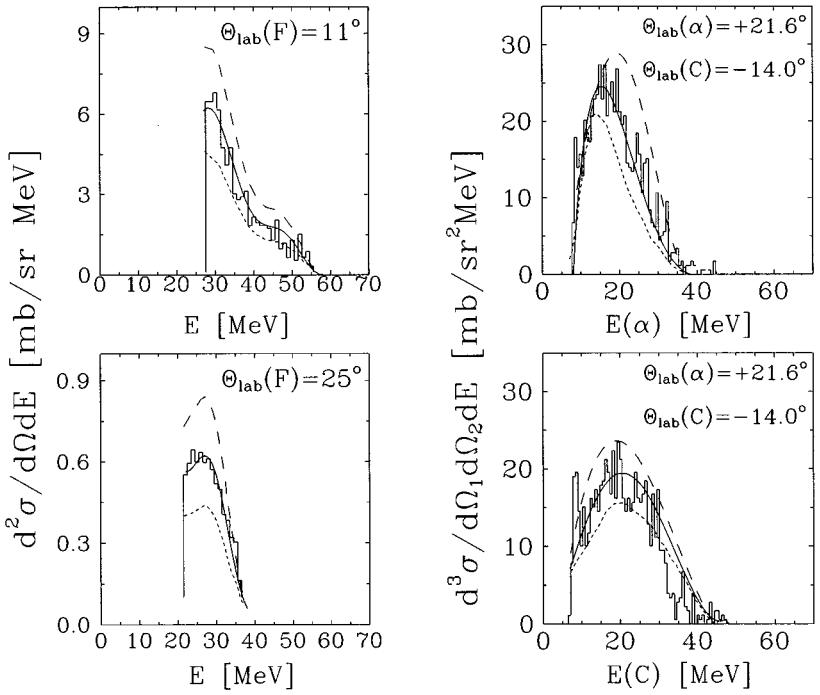

FIG. 13. Comparison of the experimental energy spectra (histograms) with the Hauser-Feshbach model calculations performed with the σ_{fus} parameter value equal to 800 mb, 850 mb, and 750 mb (solid, long-dashed, and short-dashed lines, respectively) for the F nuclei emitted at $\theta_{\mathrm{lab}} = 11°$ and 25° at $E_{\mathrm{lab}}=70$ MeV, left column, while for coincidence measurement, right column. α-C coincidence energy spectra are projected on α particle energy axis (up) and on carbon nuclei energy axis (down).

ishes, which invalidates the condition necessary for fusion [33].

The other models specify the properties of the compound nucleus as the most important factor for the limitation of the fusion. According to them the presence of a sufficiently high density of states of the compound nucleus at a given excitation energy and angular momentum (i.e., achieving by the compound system the so-called ''statistical yrast line'' [37–39]) and the stability of the virtually formed compound system against the immediate decay into smaller parts (existence of nonvanishing fission barrier for the compound system [40]) are the conditions necessary for fusion. It remains an open question which of the properties of the entrance channel and of the compound nucleus puts the most stringent constraints to the fusion and thus plays a dominant role in the limitation of the fusion cross section for the $^{12}C+^{11}B$ system. This calls for the confrontation of predictions of different models with experimental values of the fusion cross sections. In Fig. 14 the energy dependence of the experimental fusion cross sections for $^{12}C+^{11}B$ is presented together with theoretical calculations based on two entrance channel limitation models: that proposed by Wilczyński [33] (dashed line) and the model of Bass [36] (solid line). Both models are parameter free; however, the limitation imposed to fusion by the Bass model is more restrictive. As can be seen in the figure, the fusion cross sections measured in the present work (squares) agree well with both models while the former results of the Tallahassee group [7] are significantly larger than the values allowed by these two models at the highest energies. The other formulation of the entrance channel condition model as, e.g., that of Glas and Mosel [30,31] gives inconclusive results since through appropriate selection of free parameters of the model we can reproduce the fusion cross section energy dependence given by both the Wilczyński and Bass models.

The models of the fusion limitation which rely on the properties of the compound nucleus assume that a heavy-ion system, in order to fuse, must reach an effective yrast line where the compound nucleus has a sufficient level density to assure a strong absorption. This so-called ''statistical yrast line'' is shifted by some amount of excitation energy ΔQ from the yrast line of the compound nucleus. In the original paper of Lee *et al.* [37] it was proposed to assume for all systems $\Delta Q = 10$ MeV. In successive works it was found that ΔQ is proportional to the mass number of the compound nucleus $\Delta Q = 0.27 A_{\mathrm{CN}}$ [39]. The limitation of fusion cross section due to statistical yrast line for ^{23}Na compound nucleus is shown in the upper part of the Fig. 15 (the solid line for $\Delta Q = 0.27 A_{\mathrm{CN}}$, i.e., 6.2 MeV) and compared with the experimental data on the fusion cross section. As can be

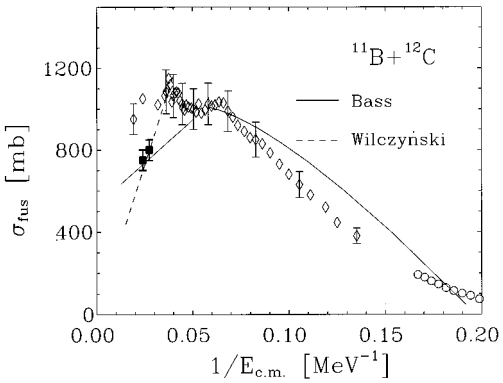

FIG. 14. The energy dependence of experimental fusion cross section for the $^{12}C+^{11}B$ system compared with predictions based on the entrance channel limitations models of Wilczyński (dashed line) and Bass (solid line). The data obtained in the present work are shown as solid squares and those from the literature as diamonds [7] and circles [42].

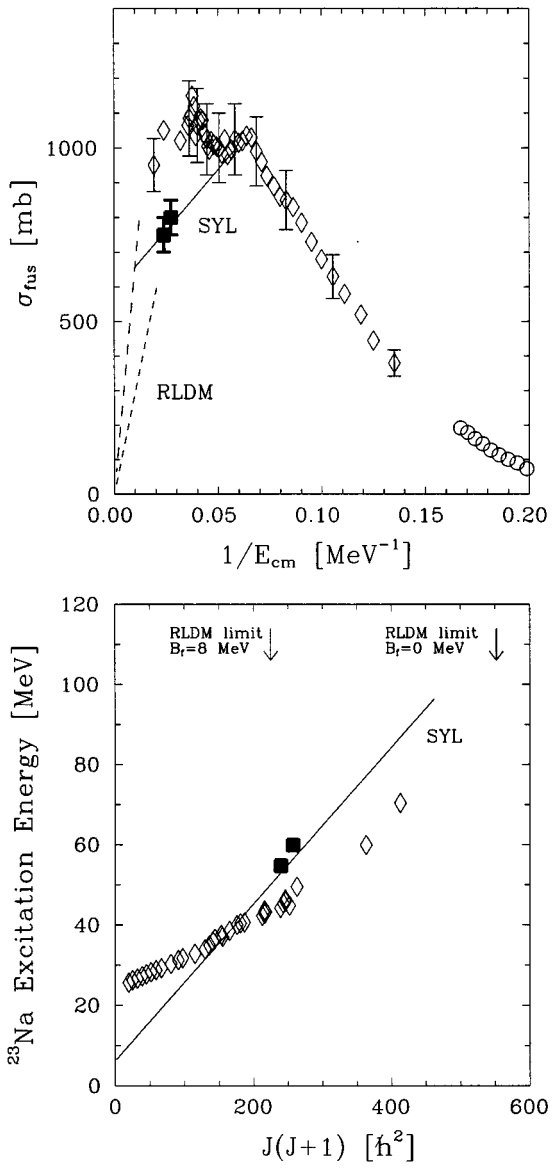

FIG. 15. The upper part: the energy dependence of the experimental fusion cross section for the $^{12}C+^{11}B$ system compared with predictions based on the compound nucleus limitations models. The solid line was calculated from the statistical yrast line (SYL) model using $\Delta Q = 6.2$ MeV; with long and short dashed lines correspond to the limitation of the fusion cross section by the fission process with a vanishing height of the barrier and with an 8 MeV fission barrier, respectively. The lower part: the excitation energies of the compound nucleus ^{23}Na as a function of squared fusion angular momentum obtained from experiments compared with the limitation imposed by the statistical yrast line ''SYL'' calculated with $\Delta Q = 6.2$ MeV (solid line). In both parts the solid squares show the data from the present experiment and diamonds those from Ref. [7].

seen the fusion cross sections measured in the present work agree also well with the limitation requested by the statistical yrast line.

The same experimental data are shown in another representation in the lower part of Fig. 15. In this representation the data points show the excitation energy of the compound nucleus achieved during the fusion process as a function of the square of the fusion angular momentum l_{fus} defined as that limiting the fusion cross section. The statistical yrast line ''SYL'' (for $\Delta Q = 6.2$ MeV) shows the lowest excitation energies of the ^{23}Na compound nucleus allowed for given angular momenta. In this representation the limitation put to the fusion is even more pronounced than in the former one. Again, the experimental points obtained in the present work fulfill the condition requested by the statistical yrast line.

Another limitation of the high energy fusion cross sections is caused by the instability of the compound nucleus against fission at high angular momenta and high excitation energies [40]. This limitation is shown in the upper part of Fig. 15 by short and long dashed lines. The former line corresponds to a complete vanishing of the fission barrier as calculated in the frame of the liquid drop model [41]. The latter corresponds to fission barrier of the height of 8 MeV, i.e., such that is comparable to the separation energy of light particles (nucleons and α particles) and therefore it causes the fission of the compound system to compete strongly with the emission of light particles. As can be seen in Fig. 15 the fusion cross sections, measured in the present work, are within the values allowed by this limitation.

IV. SUMMARY

The reactions in the $^{12}C+^{11}B$ system have been investigated at $E_{lab}(^{11}B) = 70$ and 80 MeV where a decrease of the fusion cross section due to some fusion limitation should appear. The inclusive spectra of protons, α particles, and Li, Be, B, C, N, O, F, and Ne ejectiles as well as coincidence spectra of proton or α particles with heavier ejectiles have been measured for several angular configurations.

In order to extract values of the fusion cross sections an extended Hauser-Feshbach analysis was performed for all obtained data including both inclusive spectra as well as coincidence ones. Fixing the parameters of the optical model and level density formula at values taken from the literature, the only free parameter to be found in the analysis was the fusion cross section. This procedure allowed us to extract precise values of the fusion cross section: 800 $\pm$ 50 mb at $E_{lab}(^{11}B) = 70$ MeV and 750 $\pm$ 50 mb at 80 MeV. The fusion mechanism was found to be responsible for approximately 50% of the total reaction cross section value determined from optical model calculations. The large contribution of direct processes in some reaction channels seems to account for the other part of the total reaction cross section.

The fusion cross sections measured in the present work agree very well with the fusion limitation imposed by models relying on the properties of the entrance channel as well as those taking into consideration compound nucleus properties. The former results at similar energies obtained by the Tallahassee group [7] evidently overcome these fusion limitations. To achieve agreement the considerable and rather unphysical changes in the model parameters would be necessary. So, e.g., to achieve agreement with a limitation based on the concept of the ''statistical yrast line,'' its slope must be changed at about 40 MeV excitation energy of the ^{23}Na compound nucleus, which would correspond to a modi-

fication of the moment of inertia of the ^{23}Na compound nucleus. It is obscure what mechanism could be responsible for such a phenomenon.

The results of the present experiments and their careful analysis show evidently the limitation of the fusion cross section in the $^{12}C+^{11}B$ system in the energy region around 40 MeV (c.m.) in accordance with the energy dependence indicated by accepted fusion reaction models. This implies a lack of anomalous energy dependence of fusion which through some coupling could induce an abnormal behavior of the elastic and inelastic proton transfer reactions found for this system in Ref. [8].

[1] U. Mosel, Comments Nucl. Part. Phys. **9**, 213 (1981).

[2] Gomez del Campo, R. A. Dayras, J. A. Biggerstaff, D. Shapira, A. H. Snell, P. H. Stelson, and R. G. Stokstad, Phys. Rev. Lett. **43**, 26 (1979).

[3] Y. Eyal, M. Beckman, R. Chechik, Z. Frankel, and H. Stocker, Phys. Rev. C **13**, 1527 (1976).

[4] D. G. Kovar, D. F. Geesaman, T. H. Braid, Y. Eisen, W. Henning, T. R. Ophel, M. Paul, K. E. Rehm, S. J. Sanders, P. Sperr, J. P. Schiffer, S. L. Tabor, S. Vigdor, B. Zeidman, and F. W. Prosser, Jr., Phys. Rev. C **20**, 1305 (1979).

[5] B. Heusch, C. Beck, J. P. Coffin, P. Engelstein, R. M. Freeman, G. Guillaume, F. Haas, and P. Wagner, Phys. Rev. C **26**, 542 (1982).

[6] C. Beck, F. Haas, R. M. Freeman, B. Heusch, J. P. Coffin, G. Guillaume, F. Rami, and P. Wagner, Nucl. Phys. **A442**, 320 (1985).

[7] J. F. Mateja, A. D. Frawley, D. G. Kovar, D. Henderson, H. Ikezoe, R. V. F. Janssens, G. Rosner, G. S. F. Stephans, B. Wilkins, K. T. Lesko, and M. F. Vineyard, Phys. Rev. C **31**, 867 (1985), and references therein.

[8] S. Albergo, S. Costa, R. Potenza, J. Romański, C. Tuvé, L. Jarczyk, B. Kamys, A. Magiera, A. Strzałkowski, R. Barnà, V. D'Amico, D. De Pasquale, and G. Mannino, Phys. Rev. C **43**, 2704 (1991).

[9] L. Jarczyk, B. Kamys, A. Magiera, A. Strzałkowski, S. Albergo, S. Costa, R. Potenza, J. Romański, C. Tuvé, R. Barná, V. D'Amico, D. De Pasquale, and G. Mannino, Phys. Rev. C **44**, 2053 (1991).

[10] L. Jarczyk, B. Kamys, A. Magiera, Z. Rudy, A. Strzałkowski, B. Styczeń, J. Hebenstreit, W. Oelert, P. von Rossen, and H. Seyfert, Phys. Rev. C **46**, 1393 (1992).

[11] R. Barnà, V. D'Amico, D. De Pasquale, A. Italiano, A. Lamberto, L. Jarczyk, B. Kamys, M. Kistryn, A. Kozela, A. Magiera, Z. Rudy, A. Strzałkowski, S. Albergo, R. Potenza, and J. Romański, Phys. Rev. C **50**, 300 (1994).

[12] W. Hauser and H. Feshbach, Phys. Rev. **87**, 360 (1952).

[13] A. Gavron, in *Computational Nuclear Physics 2, Nuclear Reactions*, edited by K. Langanke, J. A. Maruhn, and S. E. Koonin (Springer-Verlag, Berlin, 1993), p. 108.

[14] M. Kistryn, Ph.D. thesis, Jagellonian University, 1996 (unpublished).

[15] C. M. Perey and F. G. Perey, At. Nucl. Data Tables **17**, 1 (1976).

[16] J. R. Huizenga and G. Igo, Nucl. Phys. **29**, 462 (1962).

[17] F. Ajzenberg-Selove, Nucl. Phys. **A460**, 1 (1986); **A475**, 1 (1987); **A490**, 1 (1988); **A506**, 1 (1990); **A523**, 1 (1991).

[18] P. M. Endt and C. van den Leun, Nucl. Phys. **A310**, 1 (1978).

[19] A. Gilbert and A. G. W. Cameron, Can. J. Phys. **43**, 1446 (1965).

[20] A. G. W. Cameron and R. M. Elkin, Can. J. Phys. **43**, 1288 (1965).

[21] T. D. Newton, Can. J. Phys. **34**, 804 (1956).

[22] A. E. S. Green and D. F. Edwards, Phys. Rev. **91**, 46 (1953).

[23] L. Jarczyk, B. Kamys, M. Kistryn, A. Magiera, Z. Rudy, A. Strzałkowski, R. Barnà, V. D'Amico, D. De Pasquale, A. Italiano, and M. Licandro, Phys. Rev. C **54**, 1302 (1996).

[24] R. G. Stokstad, J. Gomez del Campo, J. A. Biggerstaff, A. H. Snell, and P. H. Stelson, Phys. Rev. Lett. **36**, 1529 (1976).

[25] R. K. Bhowmik, E. C. Pollacco, N. E. Sanderson, J. B. A. England, and G. C. Morrison, Phys. Lett. **80B**, 41 (1978).

[26] B. Fernandez, C. Gaarde, J. S. Larsen, S. Pontoppidan, and F. Videbaek, Nucl. Phys. **A306**, 259 (1978).

[27] D. E. DiGregorio, J. Gomez del Campo, Y. D. Chan, J. L. C. Ford, Jr., D. Shapira, and M. E. Ortiz, Phys. Rev. C **26**, 1490 (1982).

[28] M. E. Ortiz, J. Gomez del Campo, Y. D. Chan, D. E. DiGregorio, J. L. C. Ford, D. Shapira, R. G. Stokstad, J. P. F. Sellschop, R. L. Parks, and D. Weiser, Phys. Rev. C **25**, 1436 (1982).

[29] M. M. Coimbra, R. M. Anjos, N. Added, N. Carlin Filho, L. Fante, Jr., M. C. S. Figueira, G. Ramirez, E. M. Szanto, and A. Szanto de Toledo, Nucl. Phys. **A535**, 161 (1991).

[30] D. Glass and U. Mosel, Phys. Rev. C **10**, 2620 (1974).

[31] D. Glass and U. Mosel, Nucl. Phys. **A237**, 429 (1975).

[32] J. R. Birkelund, L. E. Tubbs, J. R. Huizenga, J. N. De, and D. Sperber, Phys. Rep. C **56**, 107 (1979).

[33] J. Wilczyński, Nucl. Phys. **A216**, 386 (1973).

[34] R. Bass, Phys. Lett. **47B**, 139 (1973).

[35] R. Bass, Nucl. Phys. **A231**, 45 (1974).

[36] R. Bass, Phys. Rev. Lett. **39**, 265 (1977).

[37] S. M. Lee, T. Matsuse, and A. Arima, Phys. Rev. Lett. **45**, 165 (1980).

[38] R. Vandenbosh and A. J. Lazzarini, Phys. Rev. C **23**, 1074 (1981).

[39] O. Civitarese, B. V. Carlson, M. S. Hussein, and A. Szanto De Toledo, Phys. Lett. **125**, 22 (1983).

[40] B. N. Kalinkin, I. Z. Petkov, Acta Phys. Pol. **25**, 265 (1964).

[41] S. Cohen, F. Plasil, and W. J. Świątecki, Ann. Phys. (N.Y.) **82**, 557 (1974).

[42] M. D. High and B. Čujec, Nucl. Phys. **A278**, 149 (1977).